Electronic Supplementary Information for:

Doping of epitaxial graphene by direct incorporation of nickel adatoms

Virginia Carnevali,[1] *Laerte L. Patera,*[1,2,†] *Gianluca Prandini,*[1,‡] *Matteo Jugovac,*[1,#] *Silvio Modesti,*[1,2] *Giovanni Comelli,*[1,2] *Maria Peressi,*[1,3,*] *and Cristina Africh*[2,*]

[1] Università di Trieste - Dipartimento di Fisica, via Valerio 2, Trieste, Italy

[2] IOM-CNR Laboratorio TASC, S.S. 14 km 163.5 in AREA Science Park, Basovizza, I-34149 Trieste, Italy

[3] IOM-CNR DEMOCRITOS National Simulation Center, via Bonomea 265, I-34136 Trieste, Italy

[†] Present address: Institute of Experimental and Applied Physics, University of Regensburg, D-93053 Regensburg, Germany

[‡] Present address: École Polytechnique Fédérale de Lausanne, CH-1015 Lausanne, Switzerland

[#] Present address: Peter Grünberg Institute (PGI-6), Forschungszentrum Jülich, 52425 Jülich, Germany

***Corresponding Authors:** peressi@ts.infn.it (theory), africh@iom.cnr.it (experiments)

Ni-doping defects at different growth temperature

Figure S1 shows that the concentration of Ni-doping defects decreases when increasing the growth temperature. Epitaxial graphene preparation at 400 °C (left panel in Figure S1) results in a rather large defect density (about 1%), present both as individual dopants, as well as aggregates of few atoms. Conversely, increasing the substrate temperature towards 600°C leads to a lowering of the defect density (middle and right panel in Figure S1). In particular, the defect density estimated from Figure S1 is 0.61, 0.27 and 0.01 defects/nm^2 at 400, 520 and 630 ^{o}C, linearly decreasing with the temperature. We also notice that the defect density is on average homogenous when considering the μm scale, whereas it can vary on the nm scale.

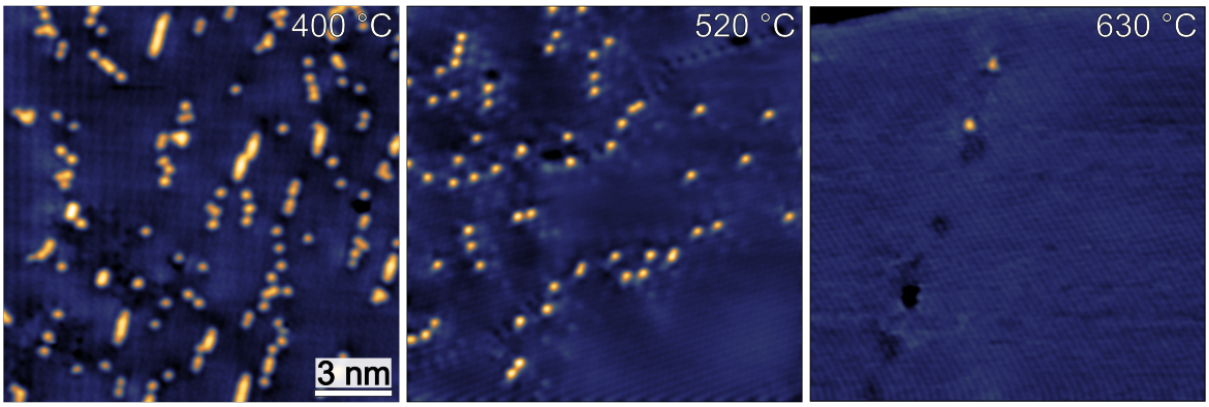

Figure S1: STM images acquired at room temperature after graphene growth at different temperatures [left panel: V_{bias} = 0.05 V, I = 0.7 nA; middle panel: V_{bias} = -0.01 V, I = 10 nA; right panel: V_{bias} = 0.02 V, I = 1.5 nA].

Apparent height of the defects

The point defects typically appear as protrusions in a wide bias range [+/- 1 V], with apparent height ranging from about 0.5 to 1.5 Å, strongly depending on the tunneling current, i.e. from the tip-sample distance (**Figure S2**). In all cases, the defect 1Ni@1V is characterized by a larger apparent height (few tens of pm) than the other species, as shown in the left panel of the Figure. This observation is in agreement with the relaxed geometry obtained by DFT, where the Ni atom is lying above the graphene plane.

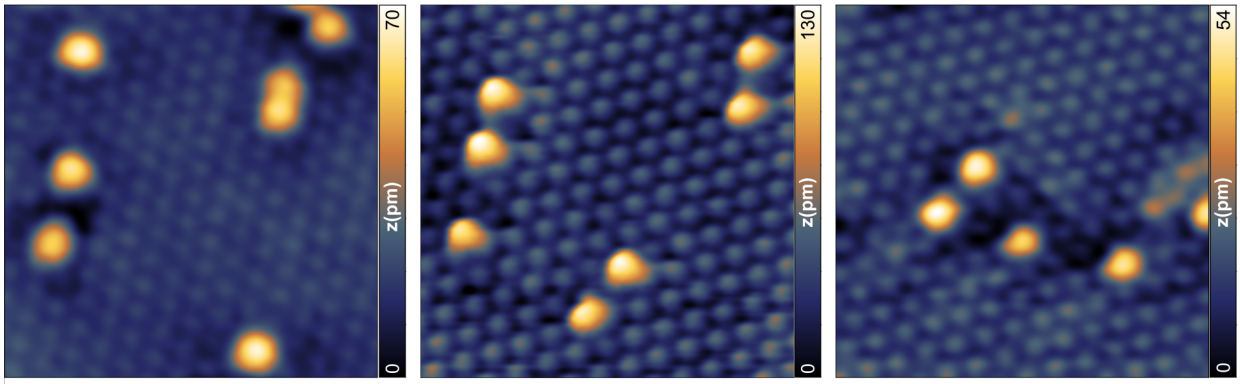

Figure S2: STM images acquired after graphene growth at different tunneling current and bias.

Ni-doped vacancies

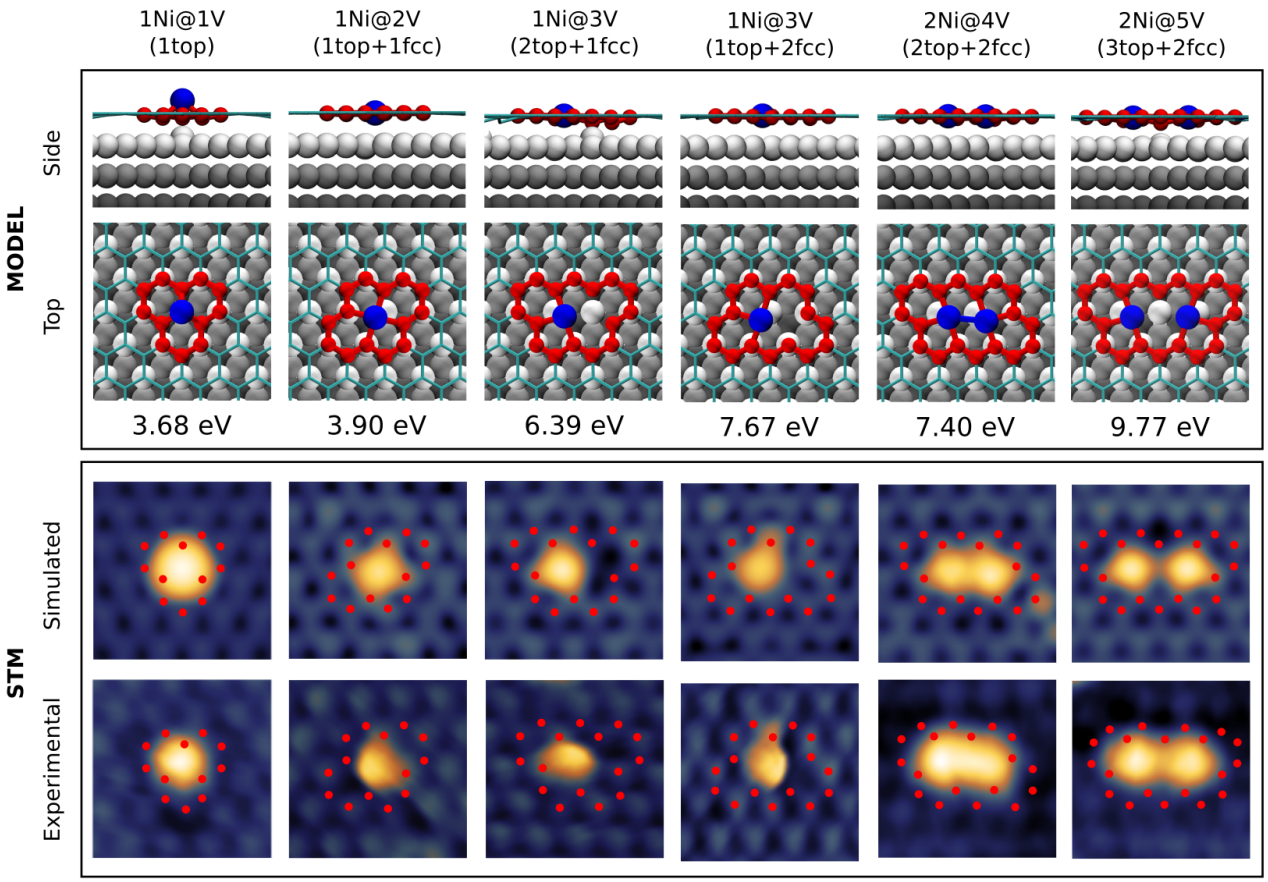

Figure S3: Ni dopant configurations in graphene on Ni(111). Same as in Figure 3 of the Main Text, but with the sketch of the C atoms delimiting the defects superimposed to the STM images, to facilitate their identification.

Ni-doping defects at different bias voltage

Figure S4 shows DFT simulated images of 1Ni@3V(2top+1fcc) at different bias voltages. The appearance remains the same in a bias range of about +/- 1 V. The same occurs also in the experimental images (see Fig. S2).

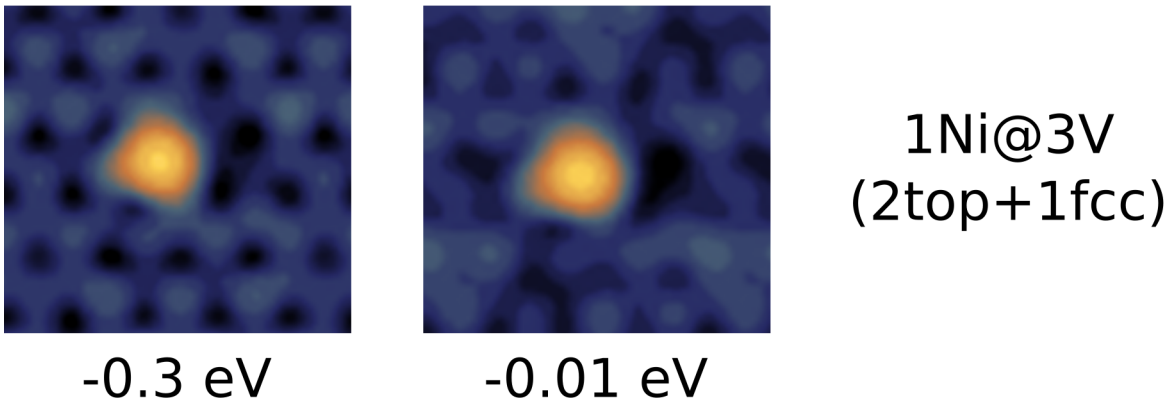

Figure S4: DFT simulated STM images of 1Ni@3V(2top+1fcc) with V_{bias}=-0.3V and V_{bias}=-0.01V; ILDOS iso-surface lying ≈2 Å above graphene and with ILDOS value of $5 \cdot 10^{-5} |e|/a_0^3$. The appearance is very similar.

1Ni@2V(1top+1fcc) defects

In the imaged area shown in **Figure S5**, all the three possible equivalent orientations of 1Ni@2V(1top+1fcc) defects are present, consistent with the identification of their atomic structure.

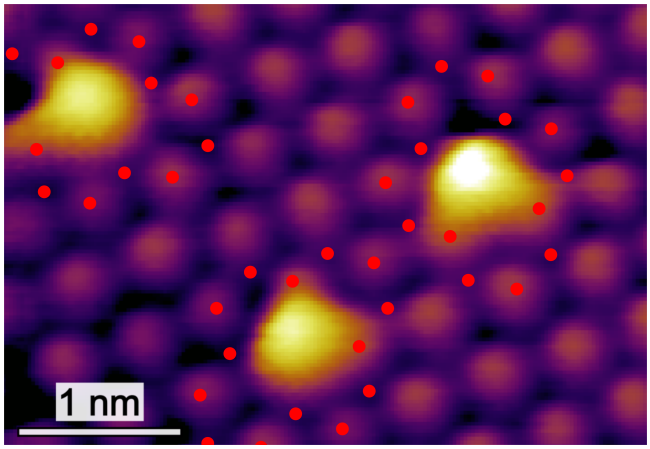

Figure S5: Different equivalent orientations of the 1Ni@2V(1top+1fcc) configuration. The sketch of the C atoms delimiting the defects is superimposed to the STM image to facilitate their identification [V_{bias} = -0.01 V, I = 8 nA].

Empty vacancies

The simulated STM images of empty vacancies reported in **Figure S6** show dark features that do not have any correspondence with the bright defects experimentally observed (see Figure 1 in the Main Text).

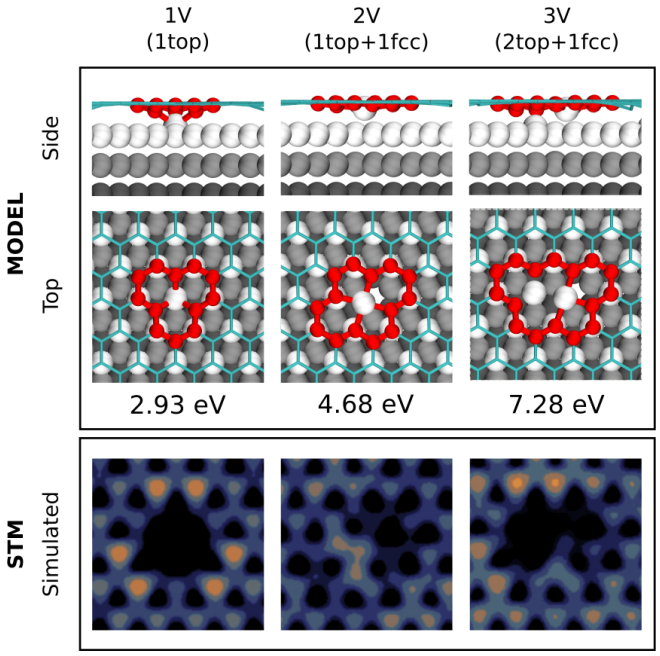

Figure S6: Empty vacancies configurations in graphene on Ni(111). The different structures are classified depending on the number and position of C vacancies (V). Top panel: stick-and-ball model of DFT relaxed structures. Formation energies are indicated below each structure. Bottom panels: DFT simulated STM images with V_{bias}=-0.3V; ILDOS iso-surface lying ≈2 Å above graphene and with ILDOS value of $5 \cdot 10^{-5} |e|/a_0^3$.

The formation energy E_{form} of the empty vacancies, calculated with reference to the pristine configurations as described in the main text, is of the same order of magnitude of the corresponding structures healed by Ni adatoms: 2.93 eV, 4.68 eV, and 7.28 eV for the 1V(1top), 2V and 3V(2top+1fcc), respectively, increasing with the number of missing C atoms. The first two values

can be compared with the findings reported in Ref. (1), i.e., with 2.80 eV for the 1V (therein indicated as 3DBs) and a value slightly higher than 4 eV for the 2V (4DBs), as can be extracted from Figure 1(i) therein.

Empty vacancies can strongly anchor the graphene layer on the substrate[2] through the passivation of the dangling bonds (DBs) with the surface atoms, in analogy with the behavior of the edges in a graphene flake.[3] The stability of the defects, once formed, can be calculated as the binding energy E_b between the defected graphene sheet and the substrate. Following Ref. (2) we define:

$$E_b = E_{def\ G/Ni} - E_G - E_{Ni\ subs}$$

where E_G and $E_{Ni\ subs}$ are the total energies of the defected graphene sheet and Ni substrate, separately relaxed to reach their equilibrium configurations. The calculated binding energies of 1V(1top), 2V and 3V(2top+1fcc) are -16.06 eV, -15.96 eV, and -17.63 eV respectively, referred to the simulation cell. For comparison with the results reported in Ref. (2) of -8.80 eV and -9.16 eV for 1V and 2V respectively, it is necessary to take into account the different cell size, including 72 C atoms in the pristine configuration in our case, and only to 24 atoms in Ref. (2). Since our cell contains additional 48 C atoms, considering a binding energy per C atom to Ni(111) of -0.16 eV in case of pristine graphene,[4] our results include an additional contribution of -7.68 eV to the binding energy, and therefore the values to be compared with Ref. (2) are -8.38 eV and -8.28 eV for 1V and 2V respectively. The residual difference could be mainly ascribed to the interaction between defects in the smaller cells and to different computational parameters.

Electronic and magnetic properties

The Ni doping affects the charge carrier concentration of the surrounding graphene region. The DFT calculated atomic charges projected onto the doping Ni adatom and the neighboring C atoms of graphene show that, in general, the Ni adatom loses electrons, whereas the surrounding C atoms gain electrons. For instance, with reference to the defects shown in **Figure S7**, we found that: in the 1Ni@2V(1top+1fcc) defect the Ni adatom loses almost 1 electron and each neighboring C atom gains 0.35 electrons; in the 1Ni@3V(1top+2fcc) defect, the Ni adatom loses almost 0.9 electrons, each C atom bond to the adatom gains 0.3-0.4 electrons, the other C atoms delimiting the defect gain 0.2 electrons.

DFT simulations indicate that, whereas surface Ni atoms are magnetic with or without a pristine epitaxial graphene overlayer above (μ = 1.05 μ_B on the bare surface and μ = 0.57 μ_B on the graphene covered Ni surface), the single trapped Ni adatom carries only a small magnetic moment (μ = 0.03-0.12 μ_B). This compares well to the findings reported for a Ni atom embedded in 1V and 2V in free-standing graphene.[5] **Figure S7** shows in details the projected density of states (PDoS) of

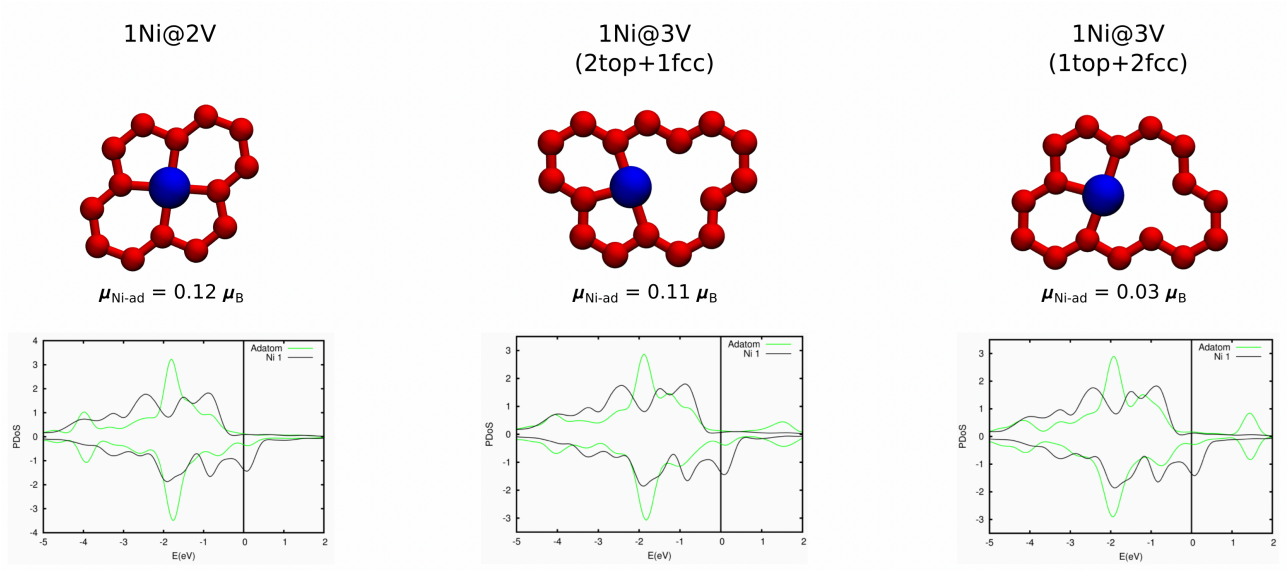

Figure S7: Upper panels: stick-and-ball model of the DFT structures of double and triple vacancies healed by a trapped Ni adatom (as in Fig. 3, but only the relevant atoms of the defect are shown). Lower panels: spin-polarized atom-projected density of states (PDoS) of the trapped Ni adatom (middle panels), compared with a Ni atom of a bare surface (labeled Ni 1).

the trapped Ni adatom. Also the magnetic moment of the surface Ni atoms underneath the defect is small, 0.02 μ_B for the one below the center of the defect. The C atoms delimiting the defect typically carry a rather small magnetization.

In order to detect magnetic fingerprints of the Ni impurities, differential conductance measurements were performed at 4.2 K with a commercial Omicron LT-STM, restricting the investigation mainly to a narrow bias window around the Fermi energy (± 50 mV). *dI/dV* spectra were acquired on roughly 50 defect sites on three different sample preparations. A marked zero-bias peak (ZBP) was detected reproducibly for all the 1Ni@2V defects investigated (about 10), being always absent for other defective structures, e.g. 1Ni@3V(2top+1fcc) and for pristine graphene (see **Figure S8**). Such feature in the *dI/dV* spectra can be potentially related to a Kondo resonance,[6] arising from the interaction between the delocalized conduction electrons in the graphene/Ni(111) surface and the magnetic impurity localized at the defect center. The presence of a Kondo state depends very critically on parameters such as the amount of hybridization between the localized defect state and the delocalized states, besides the magnetic moment of the defect.[6] This fact could be a possible justification for the absence of a Kondo peak on the 1Ni@3V(2top+1fcc) defect, which has a magnetic moment similar to that of 1Ni@2V (see Fig. S7).

The possibility of a Kondo state for the 1Ni@2V structure is intriguing because Kondo resonances of atoms or molecules on ferromagnetic substrates or contacts have been observed only in very few cases (see e.g. Refs. 7-9) and display interesting features such as possible peak splitting. However, a clear assignment of the ZBP to a Kondo resonance would definitely require additional experimental proof, such as a temperature-dependent measurement of the ZBP width at and above the Kondo temperature (~80 K as estimated from the linewidth of the peak). In parallel, a numerical investigation would require many-body techniques. A deeper investigation of the magnetic properties of the Ni-healed vacancy defects in epitaxial graphene thus clearly goes beyond the scope of this manuscript.

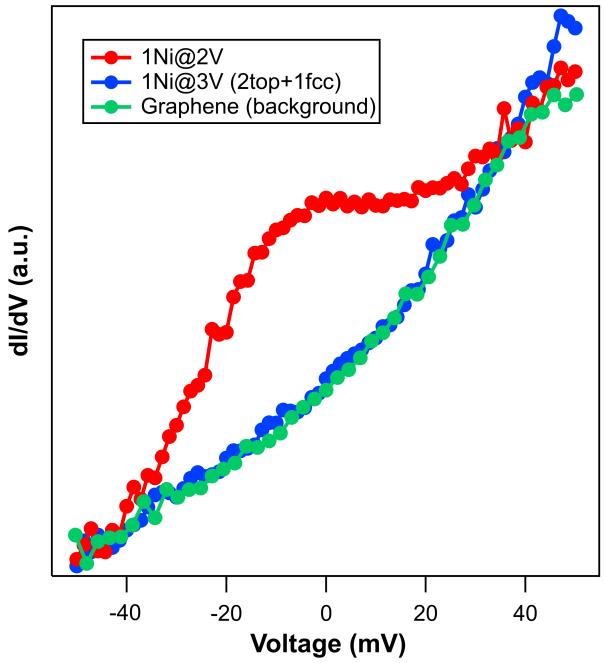

Figure S8: dI/dV spectra acquired on defective structures and on graphene [V_{mod} = 5 mV, f_{mod} = 185 Hz, T = 4.2 K].

References

(1) Wang, L.; Zhang, X.; Chan, H. L. W.; Yan, F.; Ding, F. Formation and Healing of Vacancies in Graphene Chemical Vapor Deposition (CVD) Growth. *J. Am. Chem. Soc.* **2013**, *135*, 4476–4482.

(2) Ambrosetti, A.; Silvestrelli, P. L. Toward Tunable CO Adsorption on Defected Graphene: the Chemical Role of Ni(111) and Cu(111) Substrates. *J. Phys. Chem. C* **2017**, *121*, 19828–19835.

(3) Patera, L. L.; Bianchini, F.; Troiano, G.; Dri, C.; Cepek, C.; Peressi, M.; Africh, C.; Comelli, G. Temperature-Driven Changes of the Graphene Edge Structure on Ni(111): Substrate vs Hydrogen Passivation. *Nano Lett.* **2015**, *15*, 56–62.

(4) Bianchini, F.; Patera, L. L.; Peressi, M.; Africh, C.; Comelli, G. Atomic Scale Identification of Coexisting Graphene Structures on Ni(111). *J. Phys. Chem. Lett.* **2014**, *5*, 467–473.

(5) Krasheninnikov, A. V.; Lehtinen, P. O.; Foster, A. S.; Nieminen, R. M., Pyykkö, P. Embedding Transition-Metal Atoms in Graphene: Structure, Bonding, and Magnetism. *Phys. Rev. Lett.* **2009**, *102*, 126807.

(6) Hewson, A. *The Kondo Problem to Heavy Fermions*; Cambridge University Press: Cambridge, U.K.; 1995.

(7) Pasupathy, A. N.; Bialczak, R. C.; Martinek, J; Grose, J. E.; Donev, L. A. K.; McEuen, P. L.; Ralph, D. C. The Kondo Effect in the Presence of Ferromagnetism, *Science* **2004**, *306*, 86-89.

(8) Kawahara, S. L.; Lagoute, J.; V. Repain, V.; Chacon, C.; Girard, Y.; Klein, J.; Rousset, S. Kondo Peak Splitting on a Single Adatom Coupled to a Magnetic Cluster. *Phys. Rev. B* **2010**, *82*, 020406(R) 1-4.

(9) Fu, Y-S.; Xue, Q-K.; Wiesendanger, R. Spin-Resolved Splitting of Kondo Resonances in the Presence of RKKY-Type Coupling. *Phys. Rev. Lett*. **2012** , *108*, 087203 1-5.